



THE UNIVERSITY *of* EDINBURGH

Edinburgh Research Explorer

Ultrathin composite polymeric membranes for CO₂/N₂ separation with minimum thickness and high CO₂ permeance

Citation for published version:

Javier, B, Sánchez Laínez, J, Zornoza, B, Martín, S, Carta, M, Téllez, C, Mckeown, NB, Coronas, J, Gascon, I & Malpass-Evans, R 2017, 'Ultrathin composite polymeric membranes for CO₂/N₂ separation with minimum thickness and high CO₂ permeance', *Chemsuschem*. <https://doi.org/10.1002/cssc.201701139>

Digital Object Identifier (DOI):

[10.1002/cssc.201701139](https://doi.org/10.1002/cssc.201701139)

Link:

[Link to publication record in Edinburgh Research Explorer](#)

Document Version:

Peer reviewed version

Published In:

Chemsuschem

General rights

Copyright for the publications made accessible via the Edinburgh Research Explorer is retained by the author(s) and / or other copyright owners and it is a condition of accessing these publications that users recognise and abide by the legal requirements associated with these rights.

Take down policy

The University of Edinburgh has made every reasonable effort to ensure that Edinburgh Research Explorer content complies with UK legislation. If you believe that the public display of this file breaches copyright please contact openaccess@ed.ac.uk providing details, and we will remove access to the work immediately and investigate your claim.



Ultrathin composite polymeric membranes for CO₂/N₂ separation with minimum thickness and high CO₂ permeance

Javier Benito, Javier Sánchez-Laínez, Beatriz Zornoza, Santiago Martín, Mariolino Carta, Richard Malpass-Evans, Carlos Téllez, Neil B. McKeown, Joaquín Coronas* and Ignacio Gascón*

Abstract: The use of ultrathin films as selective layers in composite membranes offers significant advantages in gas separation for increasing productivity whilst reducing the membrane size and energy costs. In this contribution, composite membranes have been obtained by the successive deposition of ca. 1 nm thick monolayers of a polymer of intrinsic microporosity (PIM) on top of dense membranes of the ultra-permeable poly[1-(trimethylsilyl)-1-propyne] (PTMSP). The ultrathin PIM films (30 nm in thickness) demonstrate CO₂ permeance up to 7 times higher than dense PIM membranes using only 0.04% of the mass of PIM without a significant decrease in CO₂/N₂ selectivity.

Polymeric membranes offer advantages in gas separation processes compared to other technologies like cryogenic distillation or selective adsorption in terms of energy efficiency.^[1] An ideal membrane should be as thin as possible, to maximize the flux (i.e. permeance) across the membrane, as selective as possible, to achieve an efficient separation, and mechanically robust.^[2] Thus, the development of ultrathin membranes (less than 100 nm) without losing selectivity is an attractive target.^[3] For composite multi-layer membranes, the cost of the polymer selective layer would be significantly reduced using ultrathin films, therefore allowing the use of high-cost, high-performance materials. This is of particular importance for large-scale gas separations such as carbon capture membrane where the required surface area of the membrane will be many square km.^[4]

Polymers of intrinsic microporosity^{[5],[6]} (PIMs) are a class of polymer with excellent performance for gas separations demonstrating both high permeability (e.g. $P_{CO_2} > 1000$ Barrer)

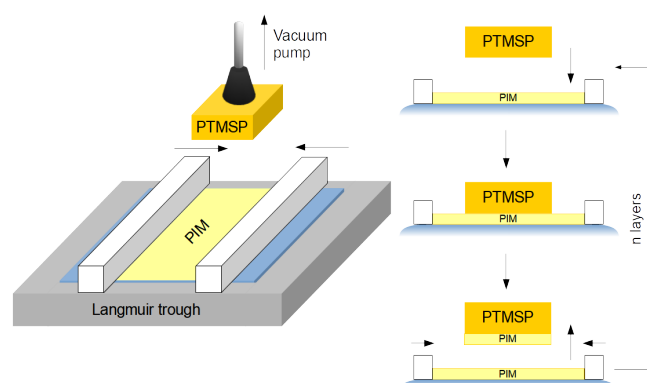
and moderate selectivity (e.g. $P_{CO_2}/P_{N_2} \sim 20$). Highly rigid PIMs composed of bridged bicyclic units such as ethanoanthracene (EA) and Troger Base (TB)^[7] are of particular interest due to their higher selectivity.

In order to obtain ultrathin layers of PIM, we considered the Langmuir-Blodgett (LB) technique^[8] which can be used for the deposition of polymeric layers on top of different kinds of supports to produce composite membranes. Using this approach, LB films formed by different surfactants have been previously deposited onto poly[1-(trimethylsilyl)-1-propyne] (PTMSP) as substrates in order to enhance selectivities for H₂/CO₂^[9] and CO₂/N₂^[10] separations. Ultrapermselective PTMSP films have been also used as support for the deposition of metal-organic covalent networks by chemical vapor deposition for gas separation membranes.^[11] Because of its extraordinarily high gas permeability,^[12] PTMSP is commonly used as gutter layer in composite membranes.^[13] Moreover, solvent cast PTMSP films present an almost flat surface and, consequently, they are very suitable supports for the deposition of selective polymer ultrathin films.

Here we report, the successive deposition of monolayers of a polymer of intrinsic microporosity, PIM-EA-TB(H₂), on top of PTMSP membranes using the Langmuir-Schaefer (LS) horizontal deposition method.^[14] We have proved that PIM-EA-TB(H₂) forms homogeneous and stable monolayers at the air-water interface that can be transferred onto different substrates using the LS method (see supporting information for further details). Each PIM-EA-TB(H₂) LS monolayer deposited had a thickness of ca. 1 nm and several monolayers could be successively deposited using this procedure (see Scheme 1) to obtain a selective layer with the desired properties.

[*] J. Benito, Dr. I. Gascón
Instituto de Nanociencia de Aragón (INA) and Departamento de Química Física
Universidad de Zaragoza
C/ Pedro Cerbuna 12, 50009 Zaragoza (Spain)
E-mail: igascon@unizar.es
J. Sánchez-Laínez, Dr. B. Zornoza, Dr. C. Téllez, Prof. Dr. J. Coronas
Instituto de Nanociencia de Aragón (INA) and Departamento de Ingeniería Química y Tecnologías del Medio Ambiente
Universidad de Zaragoza
C/ Mariano Esquillor, s/n., 50018 Zaragoza (Spain)
E-mail: coronas@unizar.es
Dr. S. Martín
Instituto de Ciencia de Materiales de Aragón (ICMA) and Departamento de Química Física
CSIC-Universidad de Zaragoza
C/ Pedro Cerbuna 12, 50009 Zaragoza (Spain)
Dr. M. Carta, Dr. R. Malpass-Evans, Prof. Dr. N. B. McKeown
School of Chemistry
University of Edinburgh
David Brewster Road, Edinburgh, EH9 3FJ (UK)

Supporting information for this article is given via a link at the end of the document.



Scheme 1. Langmuir-Schaefer horizontal deposition of PIM-EA-TB(H₂) monolayers onto PTMSP membrane. One monolayer is deposited each time that the PTMSP membrane contacts the film floating on the water surface.

Specifically, PTSMP/PIM(*n*) composite membranes, incorporating a well-defined number (*n* from 1 to 30) of PIM-EA-TB(H₂) monolayers, have been characterized and tested for CO₂/N₂ separation in post-combustion conditions (35 °C, feed pressure 1–3 bar, CO₂/N₂ mixture composition in volume 10/90). The films demonstrate a gradual increase of selectivity with *n* (Figure 1 and Table S1 of the supporting information). This procedure enabled the determination of the minimum number of PIM-EA-TB(H₂) layers required to achieve similar selectivity to that obtained from dense thick films of the selective polymer.

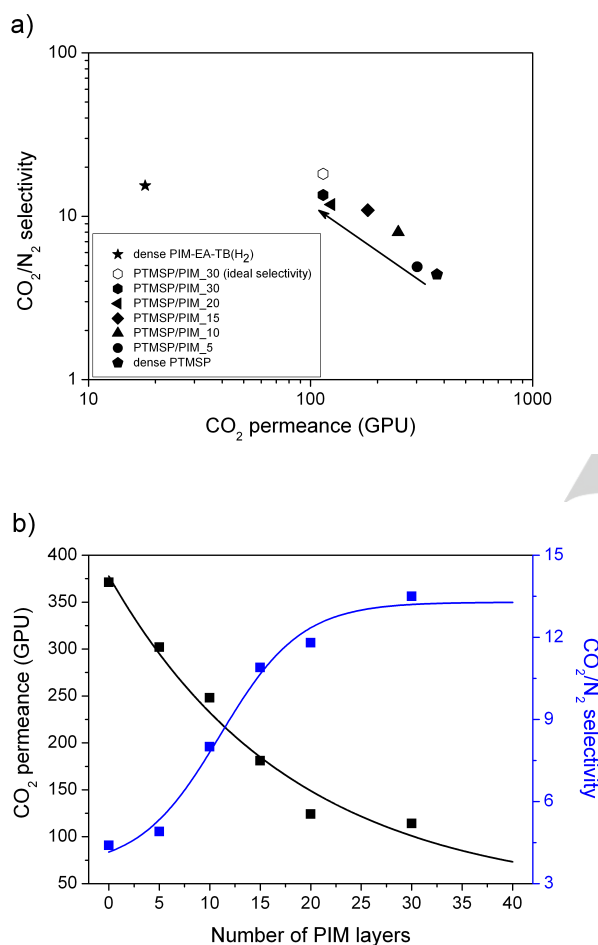


Figure 1. CO₂/N₂ separation performance of polymeric membranes studied in post-combustion conditions (CO₂/N₂ mixture composition, in volume, 10/90; 35 °C and feed pressure 3 bar). a) comparison of thick dense membranes of bare polymers and composite membranes formed by 5–30 monolayers of PIM-EA-TB(H₂) deposited onto dense PTMSP. The arrow indicates the tendency when the number of LS PIM-EA-TB(H₂) films deposited increases. b) Separation performance of polymeric membranes vs. number of PIM-EA-TB(H₂) monolayers deposited onto PTMSP. Symbols are experimental data and solid lines fitted curves using simple equations (exponential decay for CO₂ permeance and Boltzmann sigmoid function for CO₂/N₂ selectivity).

As shown in Fig. 1a, dense PTMSP membranes (thickness ca. 80 μm) showed high CO₂ permeance (371 GPU) but low CO₂/N₂ selectivity (4.4). Dense PIM-EA-TB(H₂) membranes (thickness also ca. 80 μm) showed a much lower CO₂ permeance (18

GPU) but improved CO₂/N₂ selectivity (15.4), while PTSMP/PIM_30 membranes (with thickness of selective layer = 30 nm) presented a CO₂/N₂ selectivity of 13.5 close to that of the pure PIM-EA-TB(H₂) membrane but with a significantly higher CO₂ permeance of 114 GPU. Consequently, this methodology resulted in membranes of CO₂ permeance almost 7 times larger than that of the dense PIM-EA-TB(H₂) membrane despite using only 0.04% mass of the PIM-EA-TB(H₂) relative to the dense membrane (30 nm vs. 80 μm thicknesses). Moreover, single gas permeation was also studied for the PTSMP/PIM_30 membrane. For proper comparison with previously published results, the CO₂/N₂ ideal selectivity (the ratio of single gas permeances) was also calculated, reaching a value of 18.2. This value is in good agreement with the best results published for dense membranes of the structurally similar polymer PIM-EA-TB^[15] (CO₂/N₂ selectivity values reported depend on the activation procedure and measuring device and oscillate between 13 and 19).

For membranes with a number of PIM-EA-TB(H₂) monolayers below 20, an increase in the feed pressure (Table S1 and Figure S9) caused a decrease in the CO₂/N₂ selectivity that may be related to defects in the ultrathin PIM layers. With a higher numbers of layers the selectivity remained almost constant at feed pressures between 1 and 3 bar, suggesting the achievement of an almost defect-free ultrathin selective layer, in agreement with the overall increase in the selectivity. Furthermore, a basic mathematical fitting of the composite membrane performance with the number of PIM monolayers allowed determining that 30 PIM monolayers optimize the selectivity and CO₂ permeance of composite membranes (see Figure 1b).

LS films deposited onto different solid substrates have been characterized using UV-vis and X-ray photoelectron spectroscopy (XPS), thermogravimetric analysis (TGA) and atomic force microscopy (AFM). LS films deposited onto quartz substrates show an almost constant increase of the film absorbance with the number of layers up to *n* = 30 (Figure 2) revealing a continuous and constant polymer deposition between 1 and 30 monolayers.

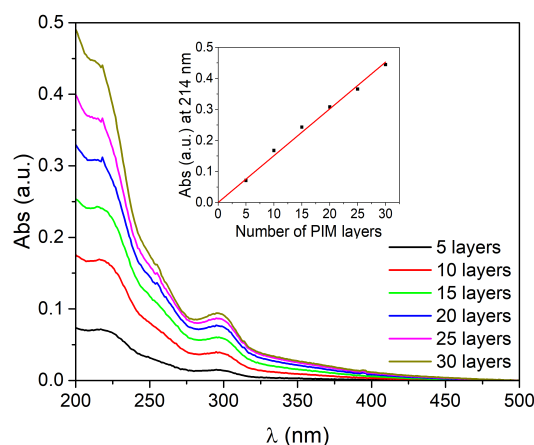


Figure 2. UV-vis spectra of PIM LS films deposited onto quartz (inset: Absorbance at λ = 214 nm vs. number of PIM-EA-TB(H₂) LS layers deposited)

Additionally, XPS spectra provided information about the elemental composition of the surface of membranes with different number of PIM-EA-TB(H₂) monolayers deposited (Table 1 and Figures S5, S6 and S7 of the supporting information). In a bare PTMSP membrane, the nitrogen content was negligible, while the silicon content was 11.7%.

Table 1. Surface atomic percentages of C, N and Si in polymeric membranes determined by XPS.

| Membrane | % C | % N | % Si |
|--------------|------|-----|------|
| bare PTMSP | 88.3 | - | 11.7 |
| PTMSP/PIM_1 | 87.9 | 3.5 | 8.6 |
| PTMSP/PIM_5 | 90.3 | 6.7 | 3.0 |
| PTMSP/PIM_10 | 90.8 | 7.6 | 1.6 |

For PTMSP/PIM_n membranes, when the number of LS layers increased from 1 to 10, the Si content gradually fell down to 1.6% at the same time that the N content increased up to 7.6% confirming the growth of the stacking of PIM-EA-TB(H₂) on top of the PTMSP membrane with each LS deposition.

AFM characterization was used to analyze the thickness and roughness of the membranes (Figure 3 and Figure S2). Bare PTMSP membranes present a root mean square roughness (RMS) of 1.06 nm. When one LS PIM-EA-TB(H₂) film was deposited, the RMS of the PTMSP/PIM₁ membrane (0.88 nm) was similar or even lower than in the pure PTMSP membrane. This confirms that the deposition of the PIM-EA-TB(H₂) monolayer did not significantly modify the textural roughness of the PTMSP membrane, allowing the deposition of successive polymer layers. Additionally, a ca. 1 nm thickness of the LS monolayer was determined measuring the height profile in different film borders (Figure 3b).

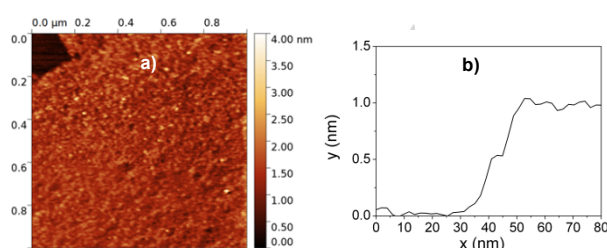


Figure 3. a) AFM characterization of PTMSP/PIM₁ composite membrane (only 1 LS PIM monolayer deposited). The thickness of the PIM-EA-TB(H₂) LS film was obtained measuring the height in different film borders as shown in b).

The density of PIM LS films has been estimated considering the molar mass of the monomer (270 g·mol⁻¹), the area per monomer at the surface pressure of transference (0.31 nm²·monomer⁻¹) and the height of the monolayer (1 nm). The value obtained (1.45 g·cm⁻³) is significantly higher than the experimental density reported for structurally similar polymer

PIM-EA-TB (1.08 g·cm⁻³)^[15] which reveals that this methodology allows the deposition of compact PIM monolayers.

To gain insight into the microscopic membrane structure, a cross-section of a PTMSP/PIM₃₀ (30 layers) sample was characterized by SEM (Figure 4a). It is possible to distinguish a coating of about 30 nm that corresponds to the stacking of 30 PIM-EA-TB(H₂) LS monolayers with a different contrast to that of the lower PTMSP dense membrane. The elemental composition of two sections of PTMSP/PIM₃₀ was analyzed by focused ion beam-scanning electron microscopy (FIB-SEM). This allows cutting the membrane with nanometer resolution (up to 5 nm) by using sputtered Ga⁺ ions in a selected area (10×5 μm in this specimen) obtaining a smooth surface. Energy-dispersive X-ray spectroscopy (EDX) was used to obtain a mapping of this sample, (Figure 4b) showing that N (green) coming from PIM-EA-TB(H₂) polymer was mainly in the upper part of the membrane while Si (red) corresponding to PTMSP was found in the bottom part.

Furthermore, a lamella of the membrane was cut for analysis by transmission electron microscopy (TEM). The sequence of images of the lamella thinning can be found in the supporting information (Figure S8). A TEM image of the lamella is depicted in Figure 4c which confirms the thickness of about 30 nm for the 30 LS layer PIM-EA-TB(H₂) film.

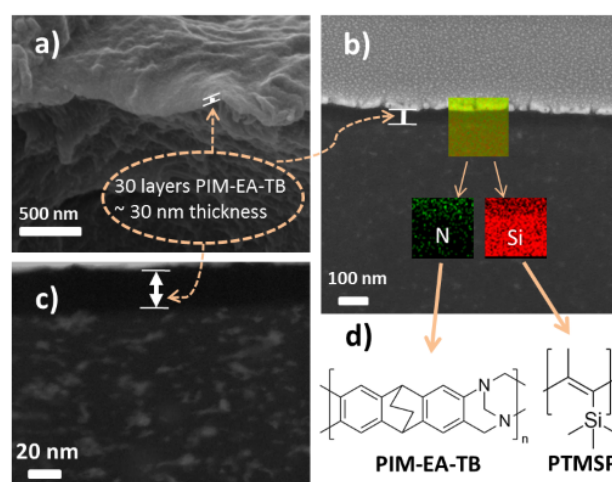


Figure 4. Electron microscopy images of the composite membrane PTMSP/PIM₃₀ with a thickness (measured in 15 different points along the sample) of 30.5±5.2 nm of PIM-EA-TB(H₂) layer (30 LS films deposited onto PTMSP): a) SEM cross-section, b) focused ion beam with an inset including an EDX mapping (N in green and Si in red), c) TEM image from a lamella extracted from the sample specimen and d) chemical structure of the polymers forming the composite membrane.

In conclusion, we have shown that using the LS method it is possible to deposit a controlled number of monolayers of a polymer of intrinsic microporosity, PIM-EA-TB(H₂), on top of PTMSP dense membranes to produce effective composite membranes for CO₂/N₂ post-combustion separation. Membranes with a selective PIM-EA-TB(H₂) layer only 30 nm thick (i.e. 0.04% of the PIM dense membrane content) present CO₂/N₂

selectivity similar to that of the dense PIM-EA-TB(H₂) with a CO₂ permeance 7 times larger.

In future works, this study will be extended to the deposition of other polymers of interest for gas separation in order to probe that this methodology can be used for different materials and processes.

Experimental Section

PIM-EA-TB(H₂) was synthesized as reported for PIM-EA-TB^[7] from 2,6(7)-diaminoanthracene by reaction with dimethoxymethane in trifluoroacetic acid. Monolayer films of PIM-EA-TB(H₂) were fabricated at the air-water interface using a commercial KSV-NIMA trough and transferred at constant surface pressure ($\pi = 30 \text{ mN}\cdot\text{m}^{-1}$) onto solid substrates (quartz, mica and PTMSP dense membranes) for characterization and CO₂/N₂ separation studies. Gas separation studies were performed by feeding a 10/90 (in volume) CO₂/N₂ mixture at 35 °C and three different feed pressures (1, 2 and 3 bar). More details about experimental procedures and results can be found in the supporting information.

Acknowledgements

The research leading to these results has received funding from the EU PF7 Programme (FP7/2007-2013), under grant agreement number 608490, project M4CO₂, Spanish MINECO and FEDER (MAT2016-77290-R) and the Aragón Government (T05). J. S.-L. thanks the MINECO for Ph.D. grant. The microscopy work was carried out in the Laboratorio de Microscopías Avanzadas at the Instituto de Nanociencia de Aragón (LMA-INA, Universidad de Zaragoza).

Keywords: Composite membranes • Gas separation • Monolayers • Polymers • Post-combustion

References

- [1] P. Bernardo, E. Drioli, G. Golemme, *Ind. Eng. Chem. Res.* **2009**, *48*, 4638-4663.
- [2] Z. Zheng, R. Grüner, X. Feng, *Adv. Mater.* **2016**, *28*, 6529-6545.
- [3] M. H. Wang, V. Janout, S. L. Regen, *Acc. Chem. Res.* **2013**, *46*, 2743-2754.
- [4] B. Seoane, J. Coronas, I. Gascon, M. E. Benavides, O. Karvan, J. Caro, F. Kapteijn, J. Gascon, *Chem. Soc. Rev.* **2015**, *44*, 2421-2454.
- [5] N. B. McKeown, P. M. Budd, *Chem. Soc. Rev.* **2006**, *35*, 675-683.
- [6] N. B. McKeown, P. M. Budd, *Macromolecules* **2010**, *43*, 5163-5176.
- [7] M. Carta, R. Malpass-Evans, M. Croad, Y. Rogan, J. C. Jansen, P. Bernardo, F. Bazzarelli, N. B. McKeown, *Science* **2013**, *339*, 303-307.
- [8] K. Ariga, Y. Yamauchi, T. Mori, J. P. Hill, *Adv. Mater.* **2013**, *25*, 6477-6512.
- [9] M. H. Wang, S. Yi, V. Janout, S. L. Regen, *Chem. Mater.* **2013**, *25*, 3785-3787.
- [10] C. Lin, Q. B. Chen, S. Yi, M. H. Wang, S. L. Regen, *Langmuir* **2014**, *30*, 687-691.
- [11] N. D. Boscher, M. H. Wang, A. Perrotta, K. Heinze, M. Creatore, K. K. Gleason, *Adv. Mater.* **2016**, *28*, 7479-7485.
- [12] T. Masuda, E. Isobe, T. Higashimura, K. Takada, *J. Am. Chem. Soc.* **1983**, *105*, 7473-7474.
- [13] Z. Dai, L. Ansaloni, L. Deng, *Green Energy & Environment* **2016**, *1*, 102-128.
- [14] J. Y. Park, R. C. Advincula, *Soft Matter* **2011**, *7*, 9829-9843.
- [15] E. Tocci, L. De Lorenzo, P. Bernardo, G. Clarizia, F. Bazzarelli, N. B. McKeown, M. Carta, R. Malpass-Evans, K. Friess, K. Pilnacek, M. Lanc, Y. P. Yampolskii, L. Strarannikova, V. Shantarovich, M. Mauri, J. C. Jansen, *Macromolecules* **2014**, *47*, 7900-7916.